

LETTERS

The association of GRB 060218 with a supernova and the evolution of the shock wave

S. Campana¹, V. Mangano², A. J. Blustin³, P. Brown⁴, D. N. Burrows⁴, G. Chincarini^{1,5}, J. R. Cummings^{6,7}, G. Cusumano², M. Della Valle^{8,9}, D. Malesani¹⁰, P. Mészáros^{4,11}, J. A. Nousek⁴, M. Page³, T. Sakamoto^{6,7}, E. Waxman¹², B. Zhang¹³, Z. G. Dai^{13,14}, N. Gehrels⁶, S. Immler⁶, F. E. Marshall⁶, K. O. Mason¹⁵, A. Moretti¹, P. T. O'Brien¹⁶, J. P. Osborne¹⁶, K. L. Page¹⁶, P. Romano¹, P. W. A. Roming⁴, G. Tagliaferri¹, L. R. Cominsky¹⁷, P. Giommi¹⁸, O. Godet¹⁶, J. A. Kennea⁴, H. Krimm^{6,19}, L. Angelini⁶, S. D. Barthelmy⁶, P. T. Boyd⁶, D. M. Palmer²⁰, A. A. Wells¹⁶ & N. E. White⁶

Although the link between long γ -ray bursts (GRBs) and supernovae has been established^{1–4}, hitherto there have been no observations of the beginning of a supernova explosion and its intimate link to a GRB. In particular, we do not know how the jet that defines a γ -ray burst emerges from the star's surface, nor how a GRB progenitor explodes. Here we report observations of the relatively nearby GRB 060218 (ref. 5) and its connection to supernova SN 2006aj (ref. 6). In addition to the classical non-thermal emission, GRB 060218 shows a thermal component in its X-ray spectrum, which cools and shifts into the optical/ultraviolet band as time passes. We interpret these features as arising from the break-out of a shock wave driven by a mildly relativistic shell into the dense wind surrounding the progenitor⁷. We have caught a supernova in the act of exploding, directly observing the shock break-out, which indicates that the GRB progenitor was a Wolf-Rayet star.

GRB 060218 was detected with the Burst Alert Telescope (BAT) instrument⁸ onboard the Swift⁹ space mission on 18.149 February 2006 Universal Time⁵. The burst profile is unusually long with a T_{90} (the time interval containing 90% of the flux) of $2,100 \pm 100$ s (Fig. 1). The flux slowly rose to the peak at 431 ± 60 s (90% containment; times are measured from the BAT trigger time). Swift slewed autonomously to the newly discovered burst. The X-ray Telescope (XRT)¹⁰ found a bright source, which rose smoothly to a peak of ~ 100 counts s^{-1} (0.3–10 keV) at 985 ± 15 s. The X-ray flux then decayed exponentially with an e -folding time of $2,100 \pm 50$ s, followed around 10 ks later by a shallower power-law decay similar to that seen in typical GRB afterglows^{11,12} (Fig. 2). The UltraViolet/Optical Telescope (UVOT)¹³ found emission steadily brightening by a factor of 5–10 after the first detection, peaking in a broad plateau first in the ultraviolet (31.3 ± 1.8 ks at 188 nm) and later in the optical (39.6 ± 2.5 ks at 439 nm) parts of the spectrum. The light curves reached a minimum at about 200 ks, after which the ultraviolet light curves remained constant while a rebrightening was seen in the optical bands, peaking again at about 700–800 ks (Fig. 2).

Soon after the Swift discovery, low-resolution spectra of the optical afterglow and host galaxy revealed strong emission lines at a redshift of $z = 0.033$ (ref. 14). Spectroscopic indications of the presence of a rising supernova (designated SN 2006aj) were found three days after the burst^{6,15} with broad emission features consistent with a type Ic supernova (owing to a lack of hydrogen and helium lines).

The Swift instruments provided valuable spectral information. The high-energy spectra soften with time and can be fitted with (cut-off) power laws. This power-law component can be ascribed to the usual GRB jet and afterglow. The most striking feature, however, is the presence of a soft component in the X-ray spectrum that is present in the XRT data up to $\sim 10,000$ s. The blackbody component shows a marginally decreasing temperature ($kT \approx 0.17$ keV, where k is the Boltzmann constant), and a clear increase in luminosity with time, corresponding to an increase in the apparent emission radius from $R_{\text{BB}}^{\text{X}} = (5.2 \pm 0.5) \times 10^{11}$ cm to $R_{\text{BB}}^{\text{X}} = (1.2 \pm 0.1) \times 10^{12}$ cm (Fig. 3). During the rapid decay ($t \approx 7,000$ s), a blackbody component is still present in the data with a marginally cooler temperature ($kT = 0.10 \pm 0.05$ keV) and a comparable emission radius: $R_{\text{BB}}^{\text{X}} = (6.5_{-4.4}^{+14}) \times 10^{11}$ cm. In the optical/ultraviolet band at 9 hours (32 ks) the blackbody peak is still above the UVOT energy range. At 120 ks the peak of the blackbody emission is within the UVOT passband, and the inferred temperature and radius are $kT = 3.7_{-0.9}^{+1.5}$ eV and $R_{\text{BB}}^{\text{UV}} = 3.29_{-0.93}^{+0.94} \times 10^{14}$ cm, implying an expansion speed of $(2.7 \pm 0.8) \times 10^9$ cm s^{-1} . This estimate is consistent with what we would expect for a supernova and it is also consistent with the line broadening observed in the optical spectra.

The thermal components are the key to interpreting this anomalous GRB. The high temperature (two million degrees) of the thermal X-ray component suggests that the radiation is emitted by a shock-heated plasma. The characteristic radius of the emitting region, $R_{\text{shell}} \approx (E/aT^4)^{1/3} \approx 5 \times 10^{12}$ cm (E is the GRB isotropic energy and a is the radiation density constant), corresponds to the radius of a blue supergiant progenitor. However, the lack of hydrogen lines

¹INAF—Osservatorio Astronomico di Brera, via E. Bianchi 46, I-23807 Merate (LC), Italy. ²INAF—Istituto di Astrofisica Spaziale e Fisica Cosmica di Palermo, via U. La Malfa 153, I-90146 Palermo, Italy. ³UCL Mullard Space Science Laboratory, Holmbury St. Mary, Dorking, Surrey RH5 6NT, UK. ⁴Department of Astronomy and Astrophysics, Pennsylvania State University, University Park, Pennsylvania 16802, USA. ⁵Università degli studi di Milano Bicocca, piazza delle Scienze 3, I-20126 Milano, Italy. ⁶NASA—Goddard Space Flight Center, Greenbelt, Maryland 20771, USA. ⁷National Research Council, 2101 Constitution Avenue NW, Washington DC 20418, USA. ⁸INAF—Osservatorio Astrofisico di Arcetri, largo E. Fermi 5, I-50125 Firenze, Italy. ⁹Kavli Institute for Theoretical Physics, UC Santa Barbara, California 93106, USA. ¹⁰International School for Advanced Studies (SISSA-ISAS), via Beirut 2-4, I-34014 Trieste, Italy. ¹¹Department of Physics, Pennsylvania State University, University Park, Pennsylvania 16802, USA. ¹²Physics Faculty, Weizmann Institute, Rehovot 76100, Israel. ¹³Department of Physics, University of Nevada, Box 454002, Las Vegas, Nevada 89154-4002, USA. ¹⁴Department of Astronomy, Nanjing University, Nanjing, 210093, China. ¹⁵PPARC, Polaris House, North Star Avenue, Swindon SN2 1SZ, UK. ¹⁶Department of Physics and Astronomy, University of Leicester, University Road, Leicester LE1 7RH, UK. ¹⁷Department of Physics and Astronomy, Sonoma State University, Rohnert Park, California 94928-3609, USA. ¹⁸ASI Science Data Center, via G. Galilei, I-00044 Frascati (Roma), Italy. ¹⁹Universities Space Research Association, 10211 Wincopin Circle Suite 500, Columbia, Maryland 21044-3431, USA. ²⁰Los Alamos National Laboratory, PO Box 1663, Los Alamos, New Mexico 87545, USA.

in the supernova spectrum suggests a much more compact source. The large emission radius may be explained in this case by the existence of a massive stellar wind surrounding the progenitor, as is common for Wolf–Rayet stars. The thermal radiation is observed once the shock driven into the wind reaches a radius, $\sim R_{\text{shell}}$, where the wind becomes optically thin.

The characteristic variability time is $R_{\text{shell}}/c \approx 200$ s, consistent with the smoothness of the X-ray pulse and the rapid thermal X-ray flux decrease at the end of the pulse. We interpret this as providing, for the first time, a direct measurement of the shock break-out^{16,17} of the stellar envelope and the stellar wind (first investigated by Colgate¹⁸). The fact that R_{shell} is larger than R_{BB}^{X} suggests that the shock expands in a non-spherical manner, reaching different points on the R_{shell} sphere at different times. This may be due to a non-spherical explosion (such as the presence of a jet), or a non-spherical wind^{19,20}. In addition, the shock break-out interpretation provides us with a delay between the supernova explosion and the GRB start of ≤ 4 ks (ref. 21; see Fig. 1).

As the shock propagates into the wind, it compresses the wind plasma into a thin shell. The mass of this shell may be inferred from the requirement that its optical depth be close to unity, $M_{\text{shell}} \approx 4\pi R_{\text{shell}}^2/\kappa \approx 5 \times 10^{-7} M_{\odot}$ ($\kappa \approx 0.34 \text{ cm}^2 \text{ g}^{-1}$ is the opacity). This implies that the wind mass-loss rate is $\dot{M} \approx M_{\text{shell}} v_{\text{wind}}/R_{\text{shell}} \approx 3 \times 10^{-4} M_{\odot} \text{ yr}^{-1}$, for a wind velocity $v_{\text{wind}} = 10^8 \text{ cm s}^{-1}$, typical for Wolf–Rayet stars. Because the thermal energy density behind a radiation-dominated shock is $aT^4 \approx 3\rho v_s^2$ (ρ is the wind density at R_{shell} and v_s the shock velocity) we have $\rho \approx 10^{-12} \text{ g cm}^{-3}$, which

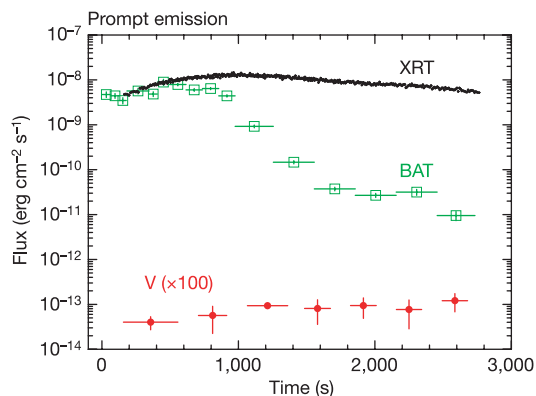


Figure 1 | Early Swift light curve of GRB 060218. GRB 060218 was discovered by the BAT when it came into the BAT field of view during a pre-planned slew. There is no emission at the GRB location up to $-3,509$ s. Swift slewed again to the burst position and the XRT and UVOT began observing GRB 060218 159 s later. For each BAT point we converted the observed count rate to flux (15–150 keV band) using the observed spectra. The combined BAT and XRT spectra were fitted with a cut-off power law plus a blackbody, absorbed by interstellar matter in our Galaxy and in the host galaxy at redshift $z = 0.033$. The host galaxy column density is $N_{\text{H}}^z = 5.0 \times 10^{21} \text{ cm}^{-2}$ and that of our Galaxy is $(0.9\text{--}1.1) \times 10^{21} \text{ cm}^{-2}$. Errors are at 1σ significance. At a redshift $z = 0.033$ (corresponding to a distance of 145 Mpc with $H_0 = 70 \text{ km s}^{-1} \text{ Mpc}^{-1}$) the isotropic equivalent energy, extrapolated to the 1–10,000-keV rest-frame energy band, is $E_{\text{iso}} = (6.2 \pm 0.3) \times 10^{49} \text{ erg}$. The peak energy in the GRB spectrum is at $E_p = 4.9_{-0.3}^{+0.4} \text{ keV}$. These values are consistent with the Amati correlation, suggesting that GRB060218 is not an off-axis event²⁶. This conclusion is also supported by the lack of achromatic rise behaviour of the light curve in the three Swift observation bands. The BAT fluence is dominated by soft X-ray photons and this burst can be classified as an X-ray flash²⁷. A V-band light curve is shown with red filled circles. For clarity the V flux has been multiplied by a factor of 100. Magnitudes have been converted to fluxes using standard UVOT zero points and multiplying the specific flux by the filter Full Width at Half Maximum (FWHM). Gaps in the light curve are due to the automated periodic change of filters during the first observation of the GRB.

implies that the shock must be (mildly) relativistic, $v_s \approx c$. This is similar to GRB 980425/SN 1998bw, where the ejection of a mildly relativistic shell with energy of $\approx 5 \times 10^{49} \text{ erg}$ is believed to have powered radio^{22–24} and X-ray emission⁷.

The optical–ultraviolet emission observed at an early time of $t \lesssim 10^4$ s may be accounted for as the low-energy tail of the thermal X-ray emission produced by the (radiation) shock driven into the wind. At a later time, the optical–ultraviolet emission is well above that expected from the (collisionless) shock driven into the wind. This emission is most probably due to the expanding envelope of the star, which was heated by the shock passage to a much higher temperature. Initially, this envelope is hidden by the wind. As the star and wind expand, the photosphere propagates inward, revealing shocked stellar plasma. As the star expands, the radiation temperature decreases and the apparent radius increases (Fig. 3). The radius inferred at the peak of the ultraviolet emission, $R_{\text{BB}}^{\text{UV}} \approx 3 \times 10^{14} \text{ cm}$, implies that emission is arising from the outer $\sim 4\pi(R_{\text{BB}}^{\text{UV}})^2/\kappa \approx 10^{-3} M_{\odot}$ shell at the edge of the shocked star. As the photosphere rapidly cools, this component of the emission fades. The ultraviolet light continues to plummet as cooler temperatures allow elements to recombine and line blanketing to set in, while radioactive decay causes the optical

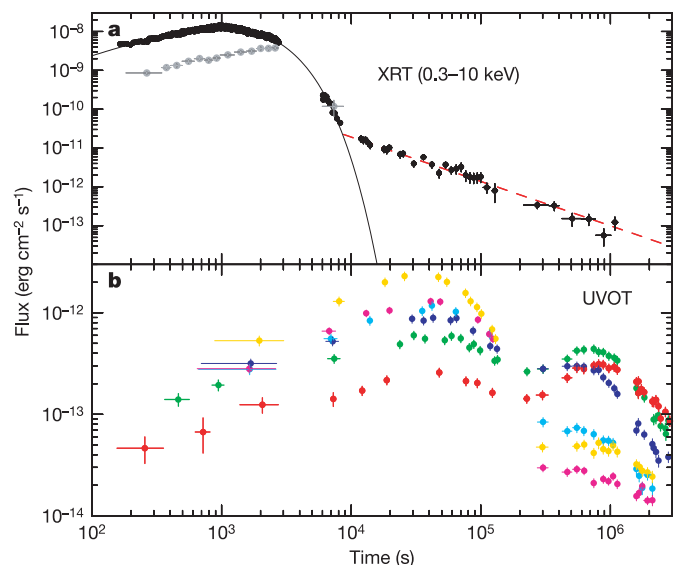


Figure 2 | Long-term Swift light curve of GRB 060218. **a**, The XRT light curve (0.3–10 keV) is shown with open black circles. Count-rate-to-flux conversion factors were derived from time-dependent spectral analysis. We also plotted (filled grey circles) the contribution to the 0.3–10-keV flux by the blackbody component. Its percentage contribution is increasing with time, becoming dominant at the end of the exponential (or steep power-law) decay. At about 10,000 s the light curve breaks to a shallower power-law decay (dashed red line) with an index of -1.2 ± 0.1 , characteristic of typical GRB afterglows. This classical afterglow can be naturally accounted for by a shock driven into the wind by a shell with kinetic energy $E_{\text{shell}} \approx 10^{49} \text{ erg}$. The t^{-1} flux decline is valid at the stage where the shell is being decelerated by the wind with the deceleration phase beginning at $t_{\text{dec}} \leq 10^4$ s for $\dot{M} \approx 10^{-4} (v_{\text{wind}}/10^8) M_{\odot} \text{ yr}^{-1}$ (where v_{wind} is in units of cm s^{-1}), consistent with the mass-loss rate inferred from the thermal X-ray component. Error bars are 1σ . **b**, The UVOT light curve. Filled circles of different colours represent different UVOT filters: red, V (centred at 544 nm); green, B (439 nm); dark blue, U (345 nm); light blue, UVW1 (251 nm); magenta, UVM1 (217 nm); and yellow, UVW2 (188 nm). Specific fluxes have been multiplied by their FWHM widths (75, 98, 88, 70, 51 and 76 nm, respectively). Data have been rebinned to increase the signal-to-noise ratio. The ultraviolet band light curve peaks at about 30 ks owing to the shock break-out from the outer stellar surface and the surrounding dense stellar wind, while the optical band peaks at about 800 ks owing to radioactive heating in the supernova ejecta.

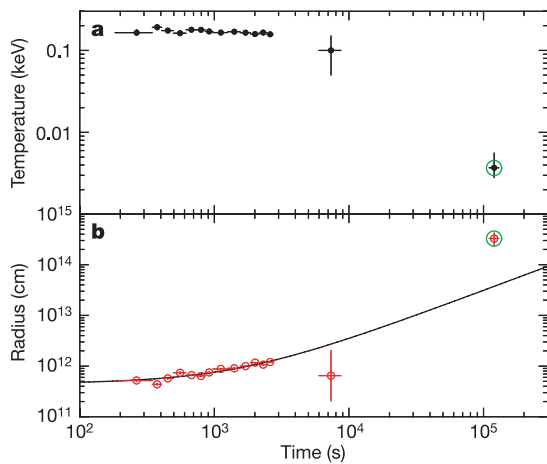


Figure 3 | Evolution of the soft thermal component temperature and radius. **a**, Evolution of the temperature of the soft thermal component. The joint BAT and XRT spectrum has been fitted with a blackbody component plus a (cut-off) power-law in the first $\sim 3,000$ s (see also the legend of Fig. 1). The last point (circled in green) comes from a fit to the six UVOT filters, assuming a blackbody model with Galactic reddening, $E(B - V) = 0.14$, and host galaxy reddening. This reddening has been determined by fitting the Rayleigh–Jeans tail of the blackbody emission at 32 ks (9 hours). The data require an intrinsic $E(B - V) = 0.20 \pm 0.03$ (assuming a Small Magellanic Cloud reddening law²⁸). Error bars are 1σ . **b**, Evolution of the radius of the soft thermal component. The last point (circled in green) comes from the fitting of UVOT data. The continuous line represents a linear fit to the data.

light to begin rising to the primary maximum normally seen in supernova light curves (Fig. 2).

Because the wind shell is clearly larger than the progenitor radius, we infer that the star radius is definitely smaller than 5×10^{12} cm. Assuming a linear expansion at the beginning (owing to light travel-time effects) we can estimate a star radius of $R_{\text{star}} \approx (4 \pm 1) \times 10^{11}$ cm. This is smaller than the radius of the progenitors of type II supernovae, like blue supergiants (4×10^{12} cm for SN 1987A, ref. 25) or red supergiants (3×10^{13} cm). Our results unambiguously indicate that the progenitor of GRB 060218/SN 2006aj was a compact massive star, most probably a Wolf–Rayet star.

Received 13 March; accepted 10 May 2005.

1. Woosley, S. E. Gamma-ray bursts from stellar mass accretion disks around black holes. *Astrophys. J.* **405**, 273–277 (1993).
2. Paczyński, B. Are gamma-ray bursts in star-forming regions? *Astrophys. J.* **494**, L45–L48 (1993).
3. MacFadyen, A. I. & Woosley, S. E. Collapsars: gamma-ray bursts and

4. explosions in ‘failed supernovae’. *Astrophys. J.* **524**, 262–289 (1999).
4. Galama, T. J. *et al.* An unusual supernova in the error box of the γ -ray burst of 25 April 1998. *Nature* **395**, 670–672 (1998).
5. Cusumano, G. *et al.* GRB060218: Swift-BAT detection of a possible burst. *GCN Circ.* **4775** (2006).
6. Masetti, N. *et al.* GRB060218: VLT spectroscopy. *GCN Circ.* **4803** (2006).
7. Waxman, E. Does the detection of X-ray emission from SN1998bw support its association with GRB980425? *Astrophys. J.* **605**, L97–L100 (2004).
8. Barthelmy, S. D. *et al.* The Burst Alert Telescope (BAT) on the SWIFT Midex Mission. *Space Sci. Rev.* **120**, 143–164 (2005).
9. Gehrels, N. *et al.* The Swift gamma ray burst mission. *Astrophys. J.* **611**, 1005–1020 (2004).
10. Burrows, D. N. *et al.* The Swift X-Ray Telescope. *Space Sci. Rev.* **120**, 165–195 (2005).
11. Tagliaferri, G. *et al.* An unexpectedly rapid decline in the X-ray afterglow emission of long γ -ray bursts. *Nature* **436**, 985–988 (2005).
12. O’Brien, P. T. *et al.* The early X-ray emission from GRBs. *Astrophys. J.* (submitted); preprint at (<http://arXiv.org/astro-ph/0601125>) (2006).
13. Roming, P. W. A. *et al.* The Swift Ultra-Violet/Optical Telescope. *Space Sci. Rev.* **120**, 95–142 (2005).
14. Mirabal, N. & Halpern, J. P. GRB060218: MDM Redshift. *GCN Circ.* **4792** (2006).
15. Pian, E. *et al.* An optical supernova associated with the X-ray flash XRF 060218. *Nature* doi:10.1038/nature05082 (this issue).
16. Ensmann, L. & Burrows, A. Shock breakout in SN1987A. *Astrophys. J.* **393**, 742–755 (1992).
17. Tan, J. C., Matzner, C. D. & McKee, C. F. Trans-relativistic blast waves in supernovae as gamma-ray burst progenitors. *Astrophys. J.* **551**, 946–972 (2001).
18. Colgate, S. A. Prompt gamma rays and X-rays from supernovae. *Can. J. Phys.* **46**, 476 (1968).
19. Mazzali, P. A. *et al.* An asymmetric, energetic type Ic supernova viewed off-axis and a link to gamma-ray bursts. *Science* **308**, 1284–1287 (2005).
20. Leonard, D. C. *et al.* A non-spherical core in the explosion of supernova SN2004dj. *Nature* **440**, 505–507 (2006).
21. Norris, J. P. & Bonnell, J. T. How can the SN-GRB time delay be measured? *AIP Conf. Proc.* **727**, 412–415 (2004).
22. Kulkarni, S. R. *et al.* Radio emission from the unusual supernova 1998bw and its association with the gamma-ray burst of 25 April 1998. *Nature* **395**, 663–669 (1998).
23. Waxman, E. & Loeb, A. A subrelativistic shock model for the radio emission of SN1998bw. *Astrophys. J.* **515**, 721–725 (1999).
24. Li, Z.-Y. & Chevalier, R. A. Radio supernova SN1998bw and its relation to GRB980425. *Astrophys. J.* **526**, 716–726 (1999).
25. Arnett, W. D. *et al.* Supernova 1987A. *Annu. Rev. Astron. Astrophys.* **27**, 629–700 (1989).
26. Amati, L. *et al.* GRB060218: $E_{p,1} - E_{\text{iso}}$ correlation. *GCN Circ.* **4846** (2006).
27. Heise, J., *et al.* in *Proceedings of ‘Gamma-Ray Bursts in the Afterglow Era’* (eds Costa, E., Frontera, F. & Hjorth, J.) 16–21 (Springer, Berlin/Heidelberg, 2001).
28. Pei, Y. C. Interstellar dust from the Milky Way to the Magellanic Clouds. *Astrophys. J.* **395**, 130–139 (1992).

Acknowledgements We acknowledge support from ASI, NASA and PPARC.

Author Information Reprints and permissions information is available at www.nature.com/reprints. The authors declare no competing financial interests. Correspondence and requests for materials should be addressed to S.C. (sergio.campana@brera.inaf.it).